Available online at www.sciencedirect.com
SCIENCE DIRECT®
Journal of Solid State Chemistry 177 (2004) 3560–3567
JOURNAL OF SOLID STATE CHEMISTRY
www.elsevier.com/locate/jssc

Synthesis and magnetic properties of the double perovskites Ln_2NaRuO_6 (Ln = La, Pr, Nd)

William R. Gemmill, Mark D. Smith, Hans-Conrad zur Loye*

Department of Chemistry and Biochemistry, University of South Carolina, 631 Sumter St., Columbia, SC 29208, USA

Received 7 April 2004; received in revised form 22 June 2004; accepted 25 June 2004
Available online 12 August 2004

Abstract

A series of double perovskite oxides, Ln_2NaRuO_6 (Ln = La, Pr, Nd), has been prepared as single crystals from acidic molten NaOH. All three oxides crystallize in the monoclinic space group $P2_1/n$ (Glazer tilt system #10, $a^-a^-b^+$), forming a 1:1 ordered rock salt lattice of the Na^+ and Ru^{5+} cations. Magnetic susceptibility measurements show evidence of antiferromagnetic correlations at temperatures below 16, 10 and 8 K for Ln_2NaRuO_6 (Ln = La, Pr, Nd), respectively.

Keywords: Crystal growth; Hydroxide flux; Double perovskite; La_2NaRuO_6; Pr_2NaRuO_6; Nd_2NaRuO_6

1. Introduction

Perovskite oxides are perhaps the most studied family of compounds in solid-state chemistry due to their inherent ability to accommodate a wide range of elemental compositions and to display a wealth of structural variations. Perovskites have the general formula ABO_3, where A typically represents a large electropositive cation and B represents a smaller transition metal or main group ion. In its ideal form, the cubic ABO_3 perovskite can be described as consisting of corner sharing BO_6 octahedra with the A cation occupying the 12-fold coordination site in the center of 8 such octahedra. The structure can also be described as resulting from the stacking of close packed [AO_3] layers in a cubic (*abc*) fashion followed by the filling of the generated octahedral sites by the B cations. The ideal double perovskite structure of the general formula $A_2BB'O_6$ is obtained when the B cation is substituted by a B' cation in an ordered 1:1 fashion, doubling the unit cell, Fig. 1.

Among the double perovskites, compounds that contain Ru(V) have been investigated extensively owing to the wide variety of potential compositions. When one considers the general formula $AA'BRu^{5+}O_6$, Ru(V) may be stabilized with A and A' representing an alkaline earth and B a trivalent cation as in A_2LnRuO_6 (A = Sr, Ba; Ln = Eu, Tm, Yb) [1,2]. Additionally, A could represent an alkaline earth and A' a lanthanide cation with B being a divalent cation as exemplified by $BaLaCoRuO_6$ [3]. Finally, it is also possible to have A and A' represent a lanthanide and B an alkali metal exemplified by the composition La_2LiRuO_6 [4,5]. Physical properties are found to vary among the known compositions of Ru(V) containing double perovskites, for example, Sr_2EuRuO_6 is a weak ferromagnet [1] while La_2LiRuO_6 orders antiferromagnetically below 30 K [5].

Recently, our group has focused on the single crystal growth of lanthanide containing oxides of platinum group metals in an effort to investigate both the structural chemistry and the magnetic properties of such compounds. In order to do so, we developed an effective synthetic approach employing molten hydroxide fluxes. The acid–base chemistry of hydroxide fluxes, described by the Lux-Flood acid–base definition [6,7], allows for a wide range of species to be present in

*Corresponding author. Fax: +1-803-777-8505.
E-mail address: zurloye@mail.chem.sc.edu (H.-C. zur Loye).

0022-4596/$ - see front matter © 2004 Elsevier Inc. All rights reserved.
doi:10.1016/j.jssc.2004.06.050

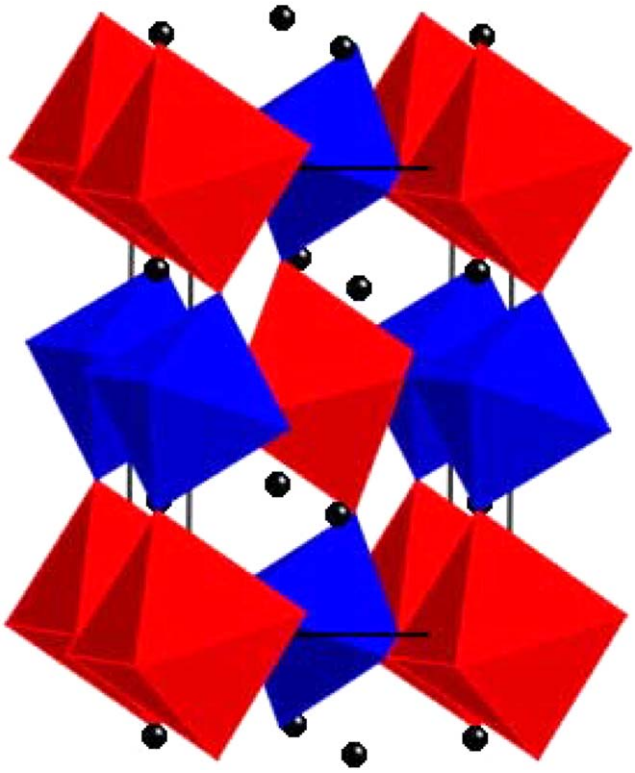

Fig. 1. Crystal structure of Ln_2NaRuO_6 (Ln = La, Pr, Nd); RuO_6 octahedra are shown in gray, NaO_6 octahedra are black, and the spheres represent Ln^{3+} cations.

solution, an essential prerequisite for their incorporation into single crystals. It is known that molten hydroxides are an excellent solvent of crystallization for lanthanide containing oxides [8,9], where the solubility of the lanthanides is dictated by the acid–base properties of the melt. Specifically, the water content of the melt must be controlled to enable the dissolution of the lanthanide oxides (Ln_2O_3's), [6,7,10] which are only soluble in acidic "wet" melts [8]. We have recently shown that such "wet" melts are one route for the growth of oxide single crystals containing both lanthanide and platinum group metals [11,12].

Coupling these two interests, we have set out to prepare lanthanide containing perovskites in which Ru(V) is stabilized, and herein we report the synthesis, structure determination, and magnetic properties of a new series of double perovskites of the general formula Ln_2NaRuO_6 (Ln = La, Pr, Nd).

2. Experimental

2.1. Crystal growth

For the title compounds, 1.00 mmol RuO_2 (synthesized from heating Ru powder (Engelhard, 99.5%) in air for 24 h), 1.00 mmol Ln_2O_3 (Alfa Aesar, Reaction, 99.9%), a 10-fold mass excess of NaOH (Fisher, ACS reagent) and 1.0 g H_2O were placed into silver tubes that had been flame sealed on one end. The silver tubes were then crimped shut on the other end, placed into a box furnace and heated to the reaction temperature of 600 °C at 10 °C/min. The reactions were held at temperature for 12 h and then cooled to 500 °C at 1 °C/min followed by turning off the furnace. The flux was dissolved with water, aided by the use of sonication, followed by manual isolation of the crystals.

2.2. Solid-state synthesis

Crystals of Pr_2NaRuO_6 could not be prepared in sufficient quantities as a phase pure sample to carry out magnetic measurements and Pr_2NaRuO_6 was, therefore, also prepared via a solid-state reaction. Polycrystalline Pr_2NaRuO_6 was prepared by mixing together 1.00 mmol RuO_2 (synthesized from heating Ru powder (Engelhard, 99.5%) in air for 24 h), 1.00 mmol Pr_2O_3 (synthesized from heating $Pr(OH)_3$ under flowing 5% H_2 in N_2 at 1000 °C for 24 h), and 0.55 mmol Na_2CO_3 (a 10% excess) were ground together and heated initially at 500 °C for 8 h after which time the temperature was increased to 900 °C and held at that temperature for 12 h. The reactant mixture was then ground and heated at 900 °C for 1 day. Further heating cycles did not change the X-ray diffraction pattern and the reaction was deemed complete after the second heat treatment.

2.3. Single crystal X-ray diffraction

For the structure determination of La_2NaRuO_6, Pr_2NaRuO_6, and Nd_2NaRuO_6, black crystals were mounted onto the end of thin glass fibers. X-ray intensity data were measured at 293(2) K on a Bruker SMART APEX diffractometer (Mo$K\alpha$ radiation, $\lambda = 0.71073$ Å) for Ln_2NaRuO_6 (Ln = La, Nd) and at 150(1) K for Pr_2NaRuO_6. The data collection covered 98.9% of reciprocal space to $2\theta = 72.7°$ (average redundancy = 2.8) for La_2NaRuO_6, 99.7% of reciprocal space to $2\theta = 70.3°$ (average redundancy = 4.0) for Pr_2NaRuO_6, and 99.9% of reciprocal space to $2\theta = 71.2°$ (average redundancy = 3.8) for Nd_2NaRuO_6. Raw area detector data frame integration and Lp corrections were carried out with SAINT+ [14]. Final unit cell parameters were determined by least-squares refinement of all reflections with $I > 5\theta(I)$ from each data set (2784 for La_2NaRuO_6, 2888 for Pr_2NaRuO_6, and 3147 for Nd_2NaRuO_6). Analysis of each data set showed negligible crystal decay during data collection. The data were corrected for absorption effects with SADABS [14].

The compounds Ln_2NaRuO_6 (Ln = La, Pr, Nd) crystallize with monoclinic symmetry in the space group $P2_1/n$ as determined by the pattern of systematic

Table 1
Crystal data and structural refinement for Ln_2NaRuO_6 (Ln = La, Pr, Nd)

Empirical formula	La_2NaRuO_6	Pr_2NaRuO_6	Nd_2NaRuO_6
Formula weight (g/mol)	497.88	501.88	508.24
Space group	$P2_1/n$	$P2_1/n$	$P2_1/n$
Unit cell dimensions			
a (Å)	5.5903(3)	5.5173(2)	5.4944(2)
b (Å)	5.9241(3)	5.9119(2)	5.9009(2)
c (Å)	7.9990(3)	7.9039(3)	7.8971(3)
β	90.495(2)°	90.786(1)°	90.883(1)°
V (Å^3)	264.90(2)	257.783(16)	255.834(16)
Z	2	2	2
Density (calculated) (mg m^{-3})	6.242	6.466	6.602
Absorption coefficient (mm$^{-1)}$	18.687	21.531	22.945
Reflections collected	3722	4719	4592
Independent reflections	1274 ($R_{int} = 0.0286$)	1138 ($R_{int} = 0.0383$)	1175 ($R_{int} = 0.0310$)
Goodness-of-fit on F^2	1.095	1.088	1.127
Final R indices [$I > 2\sigma(I)$]	$R_1 = 0.0254$, w$R_2 = 0.0582$	$R_1 = 0.0257$, w$R_2 = 0.0496$	$R_1 = 0.0247$, w$R_2 = 0.0514$
R indices (all data)	$R_1 = 0.0276$, w$R_2 = 0.0591$	$R_1 = 0.0301$, w$R_2 = 0.0507$	$R_1 = 0.0276$, w$R_2 = 0.0524$
Extinction coefficient	0.0339(4)	0.0035(4)	0.0031(4)
Residual electron density (e$^-$ Å^{-3})	1.845 and −2.444	1.716 and −2.159	1.803 and −1.693

absences in the intensity data. The structures were solved by a combination of direct methods and difference Fourier syntheses, and refined by full-matrix least-squares against F^2, with SHELXTL [15]. Refinement of the site occupation factors for the metal atoms showed no significant deviation from full occupancy in either case.

Due to the monoclinic beta angles of 90.495(2)°, 90.786(1)°, and 90.883(1)° for La_2NaRuO_6, Pr_2NaRuO_6, and Nd_2NaRuO_6, respectively, a check for pseudo-orthorhombic twinning was performed by including the twin matrix $[100/0\bar{1}0/00\bar{1}]$ in a refinement cycle. The refined twin fractions (SHELX BASF parameter) were 1.00/0.0 in each case, indicating a genuine single crystals. The twin matrix was not included in the final cycles. Relevant crystallographic data from the single-crystal structure refinements for the compounds Ln_2NaRuO_6 (Ln = La, Pr, Nd) are compiled in Table 1. For all three compounds, atomic positions and selected interatomic distances and angles are summarized in Tables 2 and 3, respectively.

2.4. Rietveld refinement of Pr_2NaRuO_6

Powder X-ray diffraction data were collected on a Rigaku D/Max-2200 powder X-ray diffractometer using a Bragg–Brentano geometry with Cu$K\alpha$ radiation. The step-scan covered the angular range 10–110° 2θ in steps of 0.02° 2θ. The diffraction data were analyzed using the Rietveld technique [16] as implemented in the EXPGUI graphical user interface [17] for GSAS [18]. Peak shapes were described by pseudo-Voigt functions and background levels were fitted by eighth-order shifted Chebyshev polynomials. The lattice parameters and atomic positions used in the initial stages of the refinement were obtained from the single crystal structure of Pr_2NaRuO_6. No significant disorder of the Na^+ and Ru^{5+} cations over the octahedral sites could be detected in trial refinements, and complete cation ordering was assumed for the final stages of the refinement. The thermal motion of all metal atoms was refined isotropically. The thermal parameters of the oxygen atoms proved unstable and were consequently fixed at 0.02 Å$^2 \times 10^3$ for the final stages of the refinement. The final observed and calculated diffraction patterns are shown in Fig. 2.

Table 2
Atomic coordinates and equivalent isotropic displacement parameters for La_2NaRuO_6, Pr_2NaRuO_6, and Nd_2NaRuO_6

	x	y	z	U(eq)
La_2NaRuO_6				
La	0.4847(1)	0.0646(1)	0.2518(1)	0.007(1)
Na	0	0	0	0.008(1)
Ru	1/2	1/2	0	0.005(1)
O_1	0.2134(4)	0.3239(4)	0.0470(3)	0.009(1)
O_2	0.6021(4)	0.4610(4)	0.2311(3)	0.009(1)
O_3	0.3302(4)	0.7787(4)	0.0583(3)	0.009(1)
Pr_2NaRuO_6				
Pr	0.4817(1)	0.0703(1)	0.2527(1)	0.005(5)
Na	0	0	0	0.006(1)
Ru	1/2	1/2	0	0.004(1)
O_1	0.2082(6)	0.3273(5)	0.0500(4)	0.006(1)
O_2	0.6136(6)	0.4518(8)	0.2318(4)	0.006(1)
O_3	0.3350(5)	0.7799(8)	0.0653(4)	0.007(1)
Nd_2NaRuO_6				
Nd	0.4811(1)	0.0710(1)	0.2529(1)	0.007(1)
Na	0	0	0	0.006(1)
Ru	1/2	1/2	0	0.005(1)
O_1	0.2076(5)	0.3272(5)	0.0506(4)	0.009(1)
O_2	0.6161(5)	0.4512(5)	0.2309(4)	0.009(1)
O_3	0.3359(5)	0.7808(5)	0.0666(4)	0.010(1)

Table 3
Selected interatomic distances (Å), bond angles (°) and tolerance factors for La_2NaRuO_6, Pr_2NaRuO_6 and Nd_2NaRuO_6

	La_2NaRuO_6	Pr_2NaRuO_6	Nd_2NaRuO_6
Ln–O(1)	2.452(2)	2.374(3)	2.366(3)
	2.702(2)	2.662(3)	2.649(3)
	2.756(2)	2.715(3)	2.710 (3)
Ln–O(2)	2.393(2)	2.342(3)	2.325(3)
	2.444(2)	2.376(3)	2.370(3)
Ln–O(3)	2.447(2)	2.401(3)	2.386(3)
	2.657(2)	2.593(3)	2.583(3)
	2.852(2)	2.863(3)	2.865(3)
Na–O(1) (× 2)	2.289(2)	2.282(3)	2.274(3)
Na–O(2) (× 2)	2.242(2)	2.237(3)	2.245(3)
Na–O(3) (× 2)	2.308(2)	2.313(3)	2.308(3)
Ru–O (× 2)	1.951(2)	1.952(3)	1.950(3)
Ru–O (× 2)	1.944(2)	1.949(3)	1.943(3)
Ru–O (× 2)	1.963(2)	1.961(3)	1.962(3)
Ru–O(1)–Na	147.61(12)	145.41(16)	145.14(15)
Ru–O(2)–Na	145.58(13)	141.39(16)	140.74(16)
Ru–O(3)–Na	144.80(13)	142.01(17)	141.40(14)
t	0.89	0.88[a]	0.87

[a]The ionic radius for Pr^{3+} in CN-12 was obtained through a linear fit extrapolation of known lanthanide element values [26].

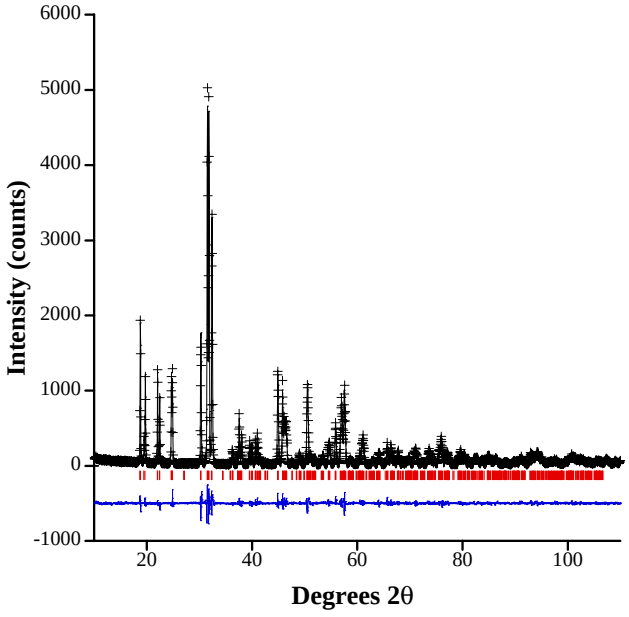

Fig. 2. Observed (+) and calculated (—) X-ray diffraction profiles of Pr_2NaRuO_6 at room temperature; a difference curve is plotted. Vertical bars mark reflection positions for the phase Pr_2NaRuO_6.

2.5. Scanning electron microscopy

Environmental scanning electron micrographs (ESEM) of several single crystals were obtained using a FEI Quanta 200 ESEM instrument utilized in the low vacuum mode. A SEM image of a representative crystal of Nd_2NaRuO_6 is shown in Fig. 3. Energy dispersive

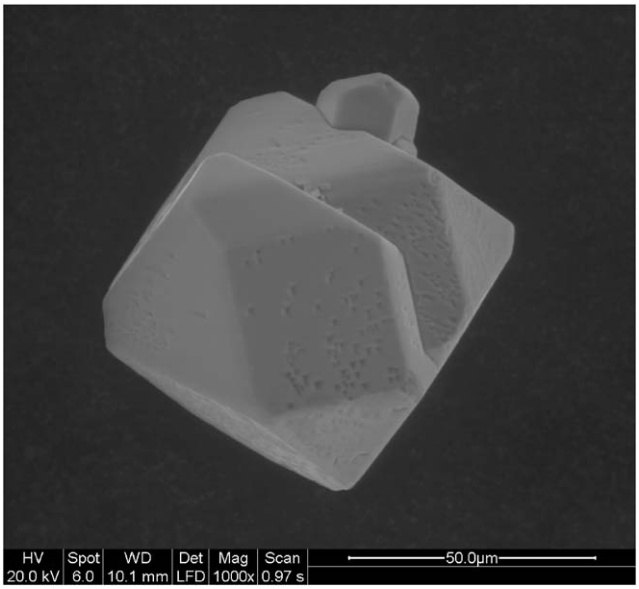

Fig. 3. SEM image of a flux grown Nd_2NaRuO_6 crystal.

spectroscopy (EDS) also verified the presence of the respective rare earth element, sodium, ruthenium, and oxygen in Ln_2NaRuO_6 (Ln = La, Pr, Nd). Within the detection limit of the instrument, no other extraneous elements were detected.

2.6. Magnetic susceptibility

The magnetic susceptibilities of the compounds Ln_2NaRuO_6 (Ln = La, Pr, Nd) were measured using a Quantum Design MPMS XL SQUID magnetometer. For the magnetic measurements, loose crystals of Ln_2NaRuO_6 (Ln = La, Nd) and polycrystalline powder of Pr_2NaRuO_6 were placed into gelatin capsules, which were placed inside plastic straws. Samples were measured under both zero-field-cooled (ZFC) and field-cooled (FC) conditions. For all measurements, the magnetization was measured in the temperature range of 2–300 K. Susceptibility measurements were carried out in an applied field of 10 kG. In addition, field sweeps were recorded between +40 and −40 kG at 100 and 2 K. The very small diamagnetic contribution of the gelatin capsule containing the sample had a negligible contribution to the overall magnetization, which was dominated by the sample signal.

3. Results and discussion

3.1. Crystal structure

Small black crystals of La_2NaRuO_6, Pr_2NaRuO_6, and Nd_2NaRuO_6 were grown from molten hydroxide fluxes

in which the flux acted as both a solvent and a reactant. Fig. 3 shows an SEM image of a flux grown crystal of Nd_2NaRuO_6 revealing the growth morphology, which is representative for crystals of this structure type, e.g., Nd_2NaIrO_6 [11]. Pr_2NaRuO_6 was prepared by standard ceramic methods due to the difficulty of isolating sufficient phase pure quantities of Pr_2NaRuO_6 crystals (black crystals of Pr_6O_{11} were always mixed with black crystals of Pr_2NaRuO_6) suitable for magnetic susceptibility measurements. The Rietveld refinement of the powder X-ray diffraction pattern of the synthesized powder, Fig. 2, demonstrated that the sample was phase pure Pr_2NaRuO_6.

The title compounds Ln_2NaRuO_6 (Ln = La, Pr, Nd) crystallize in the space group $P2_1/n$, with the monoclinic-distorted double perovskite structure type. This space group allows for a 1:1 ordered arrangement of the B and B' cations in a rock-salt type lattice and the tilting of the BO_6 and $B'O_6$ octahedra to accommodate the small size of the A cation. The Glazer tilt system assigned to the $P2_1/n$ space group is #10, $a^-a^-b^+$ [19–21]. In the title compounds, the Na^+ and Ru^{5+} cations lie on the two crystallographically independent octahedral sites while the Ln^{3+} cations occupy the A site in an eight-fold coordination environment.

It is well established that Ru(V) can be stabilized in the B site of the double perovskite structure type. The Ru–O bond distances in Ln_2NaRuO_6 (Ln = La, Pr, Nd) range from 1.949(3) to 1.963(2) and are consistent with the values observed in other Ru(V) oxides with this structure type [2,5]. The Na–O distances in Ln_2NaRuO_6 (Ln = La, Pr, Nd) range from 2.242(2) to 2.313(3) and are typical for Na^+ in an octahedral environment [11,22].

The distortion from the ideal cubic double perovskite structure for the compositions discussed in this paper is a result of the tilting of the NaO_6 and RuO_6 octahedra, while maintaining their corner sharing connectivity. This is commonly observed for compositions that include an A cation that is too small to fill the 12-fold coordination site and results in a reduced eight-fold coordination environment for the A-cation in the monoclinic structure. As both the A–O and B–O bond lengths are limited to a narrow range, the Na–O–Ru bond angles must distort. The smaller the A cation, the greater the degree of distortion of the Na–O–Ru bond angle away from the ideal 180°; consequently the β angle of the monoclinic unit cell can be considered a measure of the structure distortion. In the case of the title compounds, the β angle increases with decreasing size of the A cation, concomitantly with an increase in the deviation from the ideal 180° Na–O–Ru bond angles, as shown in Tables 1 and 4, respectively. This feature of rotated octahedra, common among all $P2_1/n$ ordered double perovskites, requires that the BO_6 and $B'O_6$ octahedra have different tilt angles as a result of the differences in size and distortion of each of the two polyhedron. These tilt angles can be calculated using a set of equations derived by Groen et al. from the cell parameters and atomic coordinates [23]. The tilt angles correspond to the rotation around the four-fold axis parallel to [001] ($w(B)$ and $w(B')$) and rotation around the two-fold axis parallel to [010] ($j(B)$ and $j(B')$) and are given in Table 4 [23]. The tilt angles corresponding to the Glazer tilt system #10 ($a^-a^-b^+$, that is two different tilts a and b) can be calculated based on the fractional positions and average M–O bond distances from the Tilting Using Backward Equations Relationship Software (TUBERS) program associated with the Structure Prediction Diagnostic Software (SPuDS) [24]. These angles are listed in Table 5. In both cases, the tilt angles increase as the Ln^{3+} cation becomes smaller across the series Ln_2NaRuO_6 (Ln = La, Pr, Nd).

Interestingly, the composition Ln_2NaRuO_6 with this structure type appears not to accept lanthanide cations smaller than Sm^{3+}. This can be rationalized using the Goldschmidt tolerance factor, t, which quantifies the relationship between the radii of the ions and the stability of the perovskite structure [13]. As in the case of the series Ln_2NaIrO_6 (Ln = La, Pr, Nd) [11], the Sm_2NaRuO_6 analogue would possess a tolerance smaller than 0.86 which appears to be the lower limit

Table 4
Calculated tilt angles for NaO_6 and RuO_6 octahedra corresponding to rotation around the four-fold axis (w(Na or Ru)) and the two-fold axis (j(Na or Ru)) parallel to [001] and [010], respectively [23]

	w(Na or Ru) Parallel to [001]	j(Na or Ru) Parallel to [010]
La_2NaRuO_6		
NaO_6	11.4°	15.9°
RuO_6	13.5°	18.4°
Pr_2NaRuO_6		
NaO_6	12.1°	18.0°
RuO_6	14.4°	20.6°
Nd_2NaRuO_6		
NaO_6	12.2°	18.2°
RuO_6	15.9°	21.0°

Table 5
Octahedral tilt angles calculated from Tilting Using Backward Equations Relationship Software (TUBERS) program associated with SPuDS [24]

Compound	Octahedral tilt angles	
	NaO_6	RuO_6
La_2NaRuO_6	17.4°	20.8°
Pr_2NaRuO_6	18.5°	22.1°
Nd_2NaRuO_6	18.7°	22.3°

for this double perovskite series. This line of reasoning is also supported by the global instability index (GII) given in the Structure Prediction Diagnostic Software (SPuDS), which reaches a value of >0.1 for the compositions Ln_2NaRuO_6 (Ln = Sm–Lu), indicating that the probability of their formation is unfavorable [24]. Experimentally we have observed that in hydroxide fluxes the smaller lanthanides samarium and europium react with ruthenium to form the fluorite-related oxide phases Ln_3RuO_7 (Ln = Sm, Eu), as discussed in our recent paper [25].

3.2. Magnetism

The temperature dependence of the magnetic susceptibility for La_2NaRuO_6 in an applied field of 10 kG is shown in Fig. 4. Fitting the high temperature susceptibility data ($100 < T > 300$) to the Curie–Weiss law results in values of $\mu_{eff} = 3.75\,\mu_B$, $\theta = -67$ K which is in good agreement with the spin only value of the d^3 Ru(V) cation of $3.87\,\mu_B$. The negative Weiss constant is indicative of antiferromagnetic correlations and the plot of the susceptibility as a function of temperature does indeed show a downturn at ~16 K, that likely indicates the onset of antiferromagnetic order. The field dependence of the magnetization was recorded at 2 K and showed no hysteresis.

The temperature dependence of the magnetic susceptibility of Pr_2NaRuO_6 measured in an applied field of 10 kG is shown in Fig. 5. The plot exhibits a ferromagnetic-like increase in the susceptibility with an onset temperature of ~20 K. It is worth noting that the magnetic susceptibility data collected at lower fields show that the ZFC and FC data no longer overlay below 10 K, where the ZFC data reaches a maximum. Fitting the high temperature susceptibility data ($100 < T > 300$) to the Curie–Weiss law results in values of $\mu_{eff} = 6.38\mu_B$, $\theta = -35$ K, which is in good agreement with the theoretical value ($6.37\,\mu_B$). This good agreement supports the assumption that Pr_2NaRuO_6 is composed of Pr^{3+} and Ru^{5+}, rather than of Pr^{4+} and Ru^{3+}. Perhaps more importantly, the double perovskite tolerance factor for Pr_2NaRuO_6 with Pr^{4+} and Ru^{3+} would be quite unfavorable.

Fig. 6 shows the field dependence of the magnetization recorded at 100 and 2 K. At 100 K, the plot is linear indicating paramagnetic behavior. At 2 K, however, a field dependence reminiscent of a soft ferromagnet with a very small hysteresis is observed. The low moment indicates that the material is not fully ferromagnetic and suggests that the material is a canted antiferromagnet instead.

The temperature dependence of the magnetic susceptibility for Nd_2NaRuO_6 in an applied field of 10 kG is shown in Fig. 7. Similar to Pr_2NaRuO_6, the plot shows a ferromagnetic-like increase in the susceptibility with an onset temperature of ~18 K, and at lower fields, the ZFC and FC data do not overlay below 8 K at which point the ZFC data reaches a maximum. Fitting the high temperature susceptibility data ($100 < T > 300$) to the Curie–Weiss law results in values of $\mu_{eff} = 6.40\mu_B$, $\theta = -7$ K which is in good agreement with the theoretical value ($6.42\,\mu_B$). Fig. 8 shows field sweeps at 100 and 2 K. A soft ferromagnet-like curve is observed at 2 K, where, however, the lack of a hysteresis and the negative Weiss constant ($\theta = -7$ K) suggest that this material also is a canted antiferromagnet.

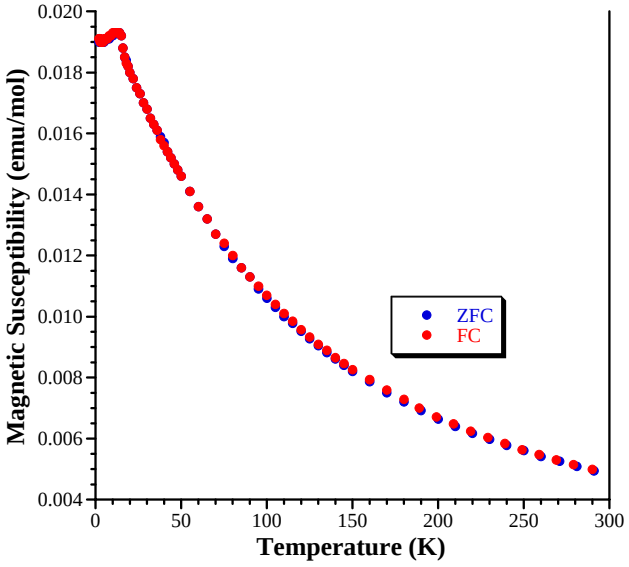

Fig. 4. Temperature dependence of the susceptibility of La_2NaRuO_6 in an applied field of 10 kG.

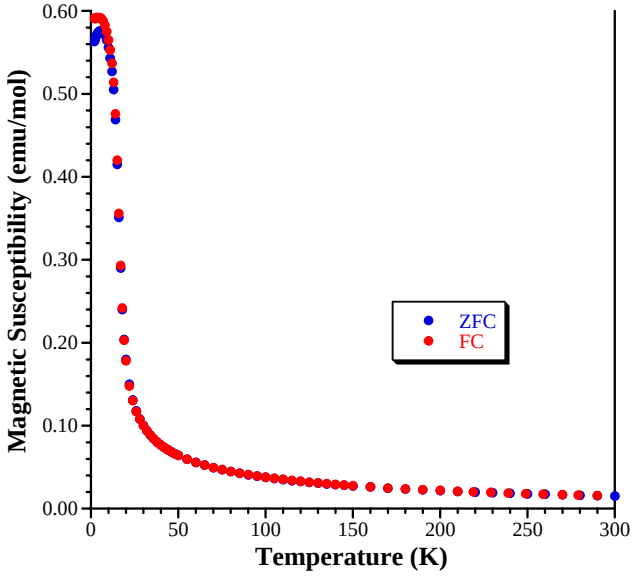

Fig. 5. Temperature dependence of the susceptibility of Pr_2NaRuO_6 in an applied field of 10 kG.

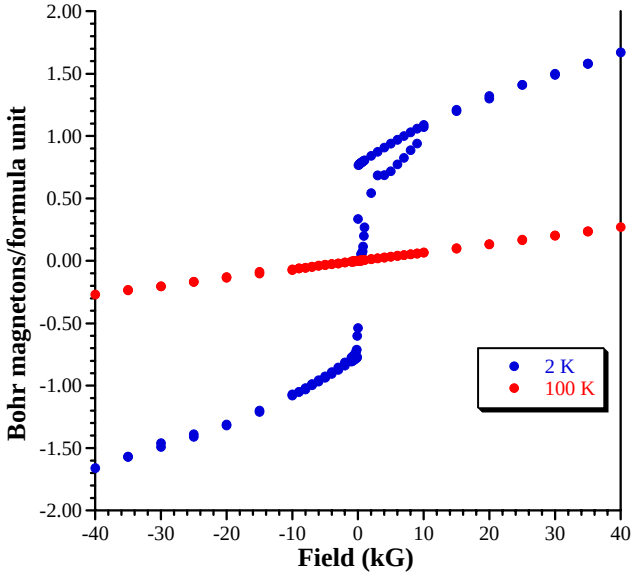

Fig. 6. Field dependence of the magnetization of Pr_2NaRuO_6 measured at 100 and 2 K.

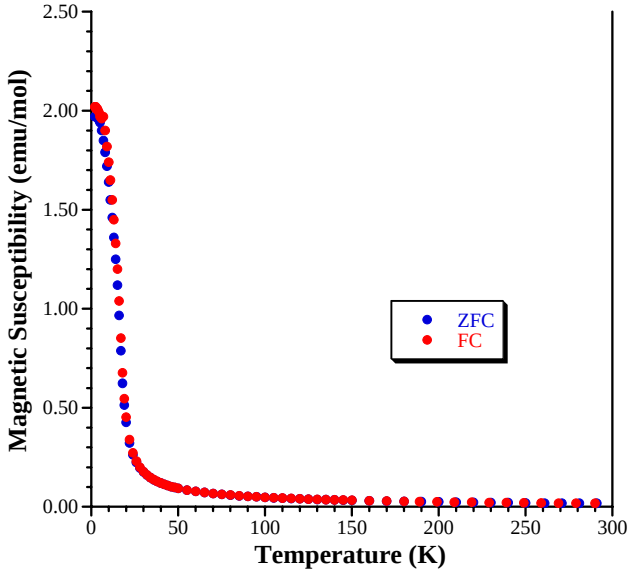

Fig. 7. Temperature dependence of the susceptibility of Nd_2NaRuO_6 in an applied field of 10 kG.

4. Conclusions

Single crystals of Ln_2NaRuO_6 (Ln = La, Pr, Nd) were prepared from reactive sodium hydroxide fluxes and a polycrystalline powder of Pr_2NaRuO_6 was prepared via standard ceramic techniques. The compounds form in the monoclinic distortion of the double perovskite structure type with a 1:1 ordered arrangement of Na^+ and Ru^{5+} cations occupying the octahedral sites. Magnetic susceptibility measurements indicate that all three compounds exhibit antiferromagnetic correlations

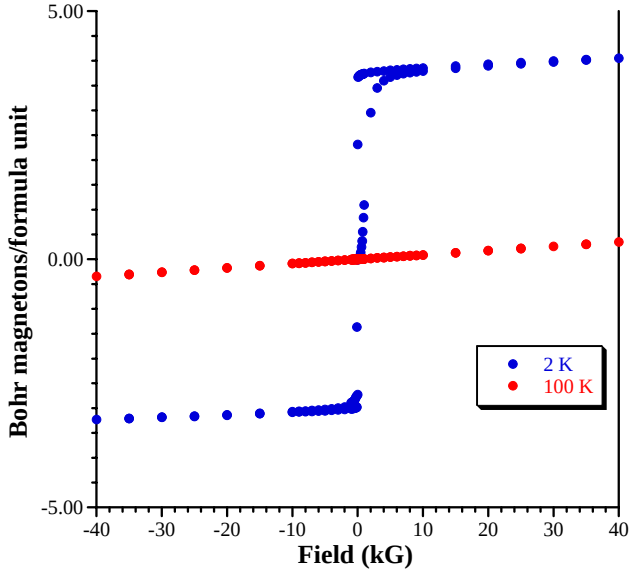

Fig. 8. Field dependence of the magnetization of Nd_2NaRuO_6 measured at 100 and 2 K.

and that Pr_2NaRuO_6 and Nd_2NaRuO_6 appear to be canted antiferromagnets.

Supplementary material

Further details of the crystal structure investigations can be obtained from the Fachinformationszentrum Karlsruhe, 76344 Eggenstein-Leopoldshafen, Germany, (fax: (49) 7247-808-666; e-mail: crystdata@fiz-karlsruhe.de) on quoting the depository numbers CSD-413921 (La_2NaRuO_6), 414148 (Pr_2NaRuO_6), and 413922 (Nd_2NaRuO_6).

Acknowledgements

Financial support for this research was provided by the National Science Foundation through the Grant DMR: 0134156. The authors would also like to thank Dr. Michael W. Lufaso for discussions concerning structural distortions in double perovskites.

References

[1] P.D. Battle, C.W. Jones, F. Studer, J. Solid State Chem. 90 (1991) 301.
[2] Y. Doi, Y. Hinatsu, A. Nakamura, Y. Ishii, Y. Morii, J. Mater. Chem. 13 (2003) 1758.
[3] P.D. Battle, T.C. Gibb, C.W. Jones, F. Studer, J. Solid State Chem. 78 (1989) 281.
[4] E.O. Oh-Kim, G. Demazeau, P. Hagenmuller, Rev. Chim. Miner. 24 (1987) 613.
[5] P.D. Battle, C.P. Grey, M. Hervieu, C. Martin, C.A. Moore, Y. Paik, J. Solid State Chem. 175 (2003) 20.
[6] H. Lux, Z. Elektrochem. 45 (1939) 303.

[7] H. Flood, T. Forland, Acta Chem. Scand. 1 (1947) 592.
[8] S.W. Keller, V.A. Carlson, D. Sanford, F. Stenzer, A.M. Stacy, G.H. Kwei, M. Alario-Franco, J. Am. Chem. Soc. 116 (1994) 8070.
[9] J.L. Luce, A.M. Stacy, Chem. Mater. 9 (1997) 1508.
[10] J. Goret, Bull. Soc. Chim. 1074 (1964).
[11] M.J. Davis, S.J. Mugavero, K.I. Glab, M.D. Smith, H.-C. zur Loye, Solid State Sci. 6 (2004) 413.
[12] M.J. Davis, M.D. Smith, H.-C. zur Loye, Inorg. Chem. 42 (2003) 6980.
[13] V.M. Goldschmidt, Naturwissenschaften 14 (1926) 477.
[14] SAINT+ Version 6.22 SMART Version 5.625, and SADABS Version 2.05. Bruker Analytical X-ray Systems, Inc., Madison, Wisconsin, USA, 2001.
[15] G.M. Sheldrick, SHELXTL Version 5.1, Bruker Analytical X-ray Systems, Inc., Madison, Madison, Wisconsin, USA, 1997.
[16] H.M. Rietveld, J. Appl. Crystallogr. 2 (1969) 65.
[17] B.H. Toby, J. Appl. Cryst. 34 (2001) 210.
[18] A.C. Larson, R.B. Von Dreele, General Structure Analysis System (GSAS). Los Alamos National Laboratory Report No. LA-UR-86-748, 1994.
[19] P.M. Woodward, Acta Crystallogr. B 53 (1997) 32.
[20] P. M Woodward, Acta Crystallogr. B 53 (1997).
[21] A.M. Glazer, Acta Crystallogr. B 28 (1972) 3384.
[22] K.E. Stitzer, M.D. Smith, H.-C. zur Loye, Solid State Sci. 4 (2002) 311.
[23] W.A. Groen, F.P.F. van Berkel, D.J.W. IJdo, Acta Crystallogr. C 42 (1986) 1472.
[24] M.W. Lufaso, P. M Woodward, Acta Crystallogr. B 57 (2001) 725.
[25] W.R. Gemmill, M.D. Smith, H.-C. zur Loye, Inorganic Chemistry 43 (2004) 4254.
[26] R.D. Shannon, Acta Crystallogr. A 32 (1976) 751.